Synthesis and properties of the *anti* and *syn* isomers of dibenzothieno[*b*,*d*]pyrrole†‡§

Ting Qi,[ab] Yunlong Guo,[ab] Yunqi Liu,*[a] Hongxia Xi,[ab] Hengjun Zhang,[ab] Xike Gao,[ab] Ying Liu,[ab] Kun Lu,[ab] Chunyan Du,[ab] Giu Yu[a] and Daoben Zhu[a]

Received (in Cambridge, UK) 6th August 2008, Accepted 22nd September 2008
First published as an Advance Article on the web 14th October 2008
DOI: 10.1039/b813683a

A novel type of *anti* and *syn* isomers of a pentacyclic compound consisting of two thiophene rings and one pyrrole ring were efficiently synthesized from benzo[*b*]thiophene, and the *anti* isomer exhibits better charge transport and OFET properties compared with the *syn* isomer and its *N*-hexyl substitution.

The linearly fused acenes, such as pentacene, are fundamental components of organic field-effect transistors (OFETs).[1] New pentacene-like heteroacenes containing sulfur[2] or nitrogen[3] atoms have been developed to improve the solubility, stability and co-facial packing in the solid state. Recently, for the pentacyclic molecules containing both sulfur and nitrogen, we first synthesized 5,6-disubstituted diindolo[3,2-*b*:4,5-*b*′]-thiophenes (DITs).[4] The results indicate that the S–S interactions enhance the electronic transport between molecules. Thus, in this paper, we designed and synthesized heteroacenes containing two sulfur atoms and one nitrogen atom, increasing the S : N ratio, which may further enhance intermolecular interactions due to S–S contact. Meanwhile, we also synthesized its isomers as *anti* (***anti*-1**) and *syn* (***syn*-1**) with respect to the orientation of thiophene and pyrrole rings along the long axis of the molecule. Research on the synthesis and properties of isomers for OFETs is seldom reported. Only Müllen's[5] and Neckers'[2g] groups recently studied the field-effect property of isomers on the analogues of polyacenes having a benzo[*b*]thiophene repeat unit. In addition, we tried to synthesize their alkyl substitutions compared with their parents. Commonly, the hexyl side chain is favorable for charge transport due to its better self-organization,[6] so we selected the hexyl group as a substituent. According to the different effect of isomers and alkyl substitution, we studied the relationship of their structure and properties, which is important for the improvement of OFET materials.

Our strategy to construct the *N*-bridged ladder bibenzo[*b*]-thiophene skeleton is based on the Cadogan reaction[7] to realize the ultimate nitrogen cyclization. Facile and efficient synthetic routes to ***anti*-1**, ***syn*-1** and **7**, their properties, and the preliminary results of field-effect transistor (FET) characteristics of their evaporated thin films are reported.

The synthetic routes to the isomers ***anti*-1**, ***syn*-1** and **7** are outlined in Scheme 1. Their starting material is benzo[*b*]thiophene which is commercially available. Notably, ***anti*-1** was obtained easily in three-step reaction sequences according to Scheme 1. The homo-coupling reaction of benzo[*b*]thiophene in the 2-position may take place in the presence of *n*-butyllithium and $CuCl_2$ at reflux in diethyl ether.[8] The next mono-substituted nitration reaction of 2,2′-bibenzo[*b*]thiophene (**2**) was carried out using 2 equiv. fuming nitric acid to produce 3-nitro compound **3** in high yield. Effective reductive cyclization of nitro **3** occurred when reflux in *o*-DCB using a slight excess of triphenylphosphine. The pure product ***anti*-1** was obtained easily by column chromatography and precipitation in 78% final yield. The synthesis of ***syn*-1** was accomplished in a similar four-step procedure (Scheme 1). Differently, 3-bromobenzo[*b*]thiophene (**4**) was at first formed by brominating with NBS directly to ensure the homo-coupling reaction in the 3-position.[9] Then, the reaction may take place in the presence of *n*-butyllithium and $CuCl_2$ at −78 °C in diethyl ether,[10] because benzo[*b*]thiophene is more active in the 3-position at low temperature.[11] The final product ***syn*-1**

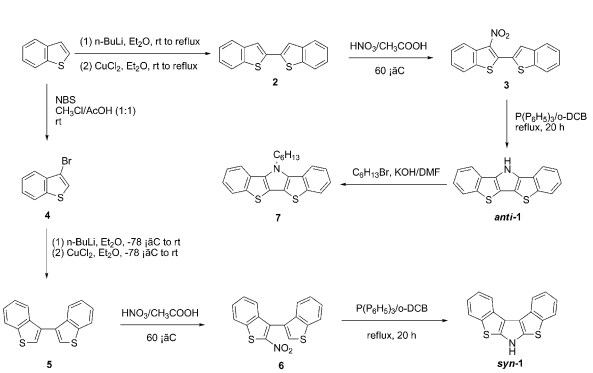

Scheme 1 Syntheses of ***anti*-1** and ***syn*-1**.

[a] *Beijing National Laboratory for Molecular Sciences, Key Laboratory of Organic Solids, Institute of Chemistry, Chinese Academy of Sciences, Beijing, 100190, China. E-mail: liuyq@iccas.ac.cn*
[b] *Graduate School of Chinese Academy of Sciences, Beijing, 100190, China*

† Electronic supplementary information (ESI) available: Synthesis, single-crystal X-ray analysis of ***anti*-1** and **7**, physicochemical properties, X-ray diffraction studies, AFM studies, device fabrication and evaluation and ^1H and ^{13}C NMR spectra. CCDC 697266 and 697267. For ESI and crystallographic data in CIF or other electronic format see DOI: 10.1039/b813683a

‡ Crystallographic data for ***anti*-1**: $C_{16}H_9NS_2$, M = 279.36, monoclinic, space group $P2_1/n$, a = 9.916(2), b = 10.619(2), c = 23.425(5) Å, V = 2453.0(8) Å^3, Z = 8, D_c = 1.513 g cm^{-3}, T = 173(2) K, reflections collected: 7940, independent reflections: 4328 (R_{int} = 0.0199), GOF = 1.168, 343 parameters, R_1 = 0.0623, wR_2 = 0.0993 for all reflections. CCDC 697266.

§ Crystallographic data for **7**: $C_{22}H_{21}NS_2$, M = 363.52, monoclinic, space group $P2_1/c$, a = 11.582(2), b = 8.1596(16), c = 19.770(4) Å, V = 1787.7(6) Å^3, Z = 4, D_c = 1.351 g cm^{-3}, T = 113(2) K, reflections collected: 12637, independent reflections: 4248 (R_{int} = 0.0717), GOF = 1.033, 227 parameters, R_1 = 0.0567, wR_2 = 0.1106 for all reflections. CCDC 697267.

was prepared by nitration and cyclization reactions from 3,3′-bibenzo[*b*]thiophene (**5**) similar to the synthetic route of ***anti*-1**. ***syn*-1** was also purified easily by column chromatography and precipitation in 51% final yield. The overall yield of ***anti*-1** was 55%, and the overall yield of ***syn*-1** was 27%. In addition, ***anti*-1** is easily alkylated in the presence of KOH to give *N*-hexyl product **7**, while the *N*-alkyl *syn* isomer cannot be obtained under same conditions.

Unexpectedly, ***anti*-1** and ***syn*-1** exhibit good solubility in common solvents. In particular, both of them can be dissolved in ethanol, and the solubility of ***anti*-1** is much better than that of ***syn*-1** at room temperature (over 20 mg ml^{-1} for ***anti*-1**, and under 2 mg ml^{-1} for ***syn*-1**). Thermogravimetric analysis revealed that ***anti*-1** has better thermal stability than ***syn*-1**, with decomposition temperatures T_d of 286 °C for ***anti*-1** and 235 °C for ***syn*-1**. The decomposition temperature T_d of *N*-hexyl *anti* isomer **7** is 296 °C, a little higher than ***anti*-1**. Notably, ***syn*-1** shows different character from ***anti*-1**, which is typical of N–H structure. Their mass spectra displayed that ***anti*-1** forms the strongest molecular ion peak, while ***syn*-1** forms the strongest fractional ion peak when a hydrogen atom leaves (ESI†), so ***syn*-1** may have the active hydrogen at the carbon near to the nitrogen. In addition, ***anti*-1** exhibits a strong IR band at 3414 cm^{-1} corresponding to N–H stretching, but ***syn*-1** exhibits no bands at 3500∼3300 cm^{-1} and a new band at 2920 cm^{-1}, characteristic of C–H stretching of saturated carbons[12] (ESI†). Therefore, we speculate that ***syn*-1** more easily forms the stable molecular structure ***syn*-1′** as shown in Scheme 2. In the ^{1}H-NMR, δ = 5.63 ppm line for ***syn*-1** in contrast to 11.94 ppm in ***anti*-1** may also verify the structure (ESI†). As aforementioned, ***syn*-1** cannot perform the *N*-alkylated reaction, which confirms this hypothesis further.

Crystals of ***anti*-1** and **7** suitable for single-crystal X-ray diffraction (XRD) studies were grown from toluene and dicholomethane, respectively. Both ***anti*-1** and **7** have dimers formed by the adjacent two molecules with anti conformation to minimize the dipolar interactions (Fig. 1b and d). Differently, the strong π–π interactions (3.41 Å for the largest plane-to-plane distance) form piled dimers for ***anti*-1**, while the strong S–S contacts (3.56, 3.21, and 3.56 Å) and interactions between alkyl chains form flatly spread dimers along the short molecular axis for **7**. Evidently, ***anti*-1** assumes the so-called sandwiched herringbone structure in which its dimers are packed tightly in the crystal (Fig. 1a). Dimers for **7**, nearly in the same plane also construct a herringbone packing pattern (Fig. 1c), but the substituted alkyl chains insert in the middle

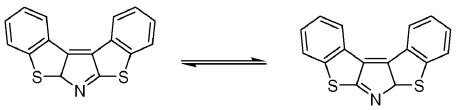

Scheme 2 The stable molecular structure ***syn*-1′**.

of parallel dimers to prevent π–π interactions between conjugated planes (ESI†). Although the mean S–S contact (3.44 Å) of **7** is shorter than that of ***anti*-1** (3.49 Å), the crystal structure of **7** does not exhibit π–π interactions that are more favorable for electronic transport. Therefore, the *anti* isomer without alkyl substituents has better charge transport structure. In the ***anti*-1** crystal, short S–S contacts (3.38, 3.51, and 3.58 Å) and C–C contacts (3.36 Å) exist between parallel slipped dimers, and short C–H···π contacts (2.66∼2.89 Å) exist in a face-to-edge manner between dimers, indicative of the two-dimensional electronic structure of the crystal.

The UV-Vis absorbance and emission spectra of ***anti*-1** display red-shifts relative to those of ***syn*-1** either in solution or in the solid state (vacuum-deposited films), and their solid-state spectra are red-shifted with respect to solution (Table 1 and ESI†). Meanwhile, at longer wavelengths, the solid-state spectrum of the thin film of ***anti*-1** shows two new peaks at 465 and 495 nm, which are attributed to intermolecular interactions in the microcrystalline film[13] and possibly related to the π–π stacking observed in the crystal. The absorbance and emission spectra of alkyl substituted *anti* isomer **7** are similar to the unsubstituted ***anti*-1** in solution. However, in the solid state, the emission maximum of **7** exhibits an obvious red shift

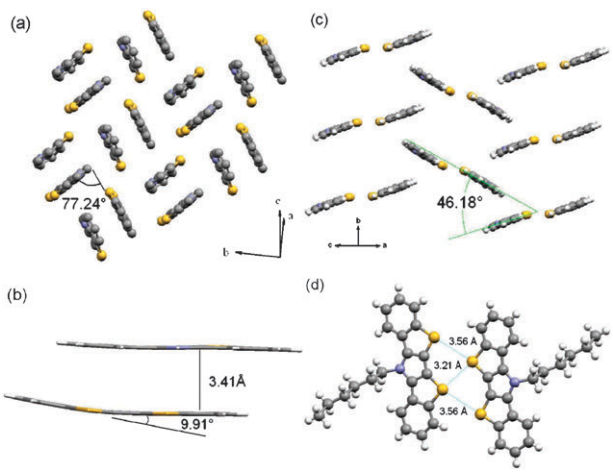

Fig. 1 Crystal structures of ***anti*-1** (a,b) and **7** (c,d), (a) hydrogen atoms removed for clarity, (c) alkyl chains removed for clarity.

Table 1 Photophysical and electrochemical data of ***anti*-1**, ***syn*-1** and **7**

	Solution					Film[d]		
Compd	λ_{abs}[a]/nm	λ_{lum}[b]/nm	E_g[c]/eV	E_{ox}[e]/V	E_{HOMO}[f]/eV	λ_{abs}/nm	λ_{lum}[b]/nm	E_g[c]/eV
***anti*-1**	327, 340	355, 365	3.51	1.02	−5.30	343, 355	402, 465, 495	3.23
***syn*-1**	286, 299, 307	356	3.71	1.53	−5.84	315	366	3.37
7	329, 345	357, 369	3.48	1.15	−5.38	337, 356	445	3.26

[a] Measured in a dilute CH_2Cl_2 solution (2×10^{-5} M). [b] Excited at the second absorption peak. [c] Estimated from the onset of absorption ($E_g = 1240/\lambda_{onset}$). [d] Films were vacuum deposited (50 nm, quartz substrate). [e] Performed in Bu_4NPF_6–CH_2Cl_2 solution (10^{-3} M), v = 100 mV s^{-1}. [f] Calculated using the empirical equation: HOMO = $-(4.44 + E_{ox}^{onset})$.

relative to ***anti*-1**, which is probably due to the extra electron donation from the alkyl groups.[14] In addition, through drop coating films, we found that ***anti*-1** can form an even and consecutive film from a toluene or ethanol solution (1 mg mL^{-1}), observing sharp absorbance band edges, but ***syn*-1** and **7** are easier to aggregate and crystallize (ESI†). This property of good film formation is seldom found in the rigid molecules without long alkyl substitution. It is a feature of ***anti*-1** that could be applied in solution processing. This work will be studied in depth.

The photostability of their vacuum-deposited thin films was studied by monitoring changes in the absorption of their thin films deposited on quartz under ambient light for nearly three months. ***syn*-1** and **7** are quite unstable, the absorption decaying to almost zero within a few days, while ***anti*-1** is very stable with no change of absorption (ESI†).

Cyclic voltammetry of ***anti*-1** and **7** showed a reversible oxidation peak at $E_{1/2} = +0.95$ V and $+1.06$ V, respectively, indicating the good stability of the ***anti*-1** and **7** radicals, while ***syn*-1** showed an irreversible oxidation peak at $E_{ox} = +1.53$ V (Ag/AgCl as reference, ESI†). The stability of the radical is an important factor in achieving high mobility,[15] so the *anti* isomer is superior to the *syn*. Given the Fc/Fc^{+} couple was used as the internal standard,[16] HOMO levels of ***anti*-1**, ***syn*-1** and **7** were estimated by using oxidation onsets -5.30, -5.84 and -5.38 eV from vacuum, respectively. It should be noted that the HOMO level of ***anti*-1** is closest to the work function of Au electrode (5.1 eV) in devices. Furthermore, the optical band gap of ***syn*-1** is too large to benefit charge transport.

Thin-film transistors of ***anti*-1**, ***syn*-1** and **7** were fabricated by vacuum evaporation in a top-contact configuration using Au as source and drain electrodes ($W/L = 3$ mm/50 μm). The devices for ***anti*-1** showed typical p-channel FET properties under ambient conditions, but the devices for ***syn*-1** and **7** showed no FET properties. The phenomenon indicates that the *anti* isomer ***anti*-1** is more favorable for charge transport than the *syn* and the alkyl substitution under the same conditions. Field-effect mobility (μ_{FET}) evaluated from the saturation regime for ***anti*-1** were of the order of 10^{-2} cm^2 V^{-1} s^{-1}, and the on/off ratio was as high as 10^5 (Table 2 and ESI†). The almost identical transistor performance acquired by repeating measurements continuously 100 times and monitoring measurements for one month showed the stability of the semiconductor under ambient conditions (ESI†).

In summary, we have established an efficient method to synthesize the *syn* (***syn*-1**) and *anti* (***anti*-1**) isomers of dibenzothieno[*b*,*d*]pyrrole and the hexyl substituted *anti* isomer (**7**), using the final reductive cyclization. Detailed studies of their physicochemical properties revealed that the *anti* isomer (***anti*-1**) has stronger intermolecular interactions than the *syn* isomer (***syn*-1**), and the *anti* has the better charge transport structure than the alkyl substitution. The HOMO energy level and photostability of ***anti*-1** are more suitable to apply in an FET device, and it can easily form an even film. The organic thin-film transistor of ***anti*-1** is fabricated and characteristic of p-type in the air. Mobility up to 0.012 cm^2 V^{-1} s^{-1} and on/off ratio up to 10^5 were achieved under ambient conditions, and the device is very stable in air. Further optimization of these transistors is underway.

Table 2 FET characteristics of devices fabricated on OTS-treated Si/SiO_2 substrates for ***anti*-1**, ***syn*-1** and **7**[a]

Compd	Mobility/cm^2 V^{-1} s^{-1}	On/off ratio	V_{th}/V
***anti*-1**	0.012	10^5	−20.8
***syn*-1**	nd[b]	nd	nd
7	nd	nd	nd

[a] Estimated from the saturation regime. [b] Not determined.

The present research was financially supported by the National Natural Science Foundation (60671047, 50673093, 60736004, 20721061), the Major State Basic Research Development Program (2006CB806203, 2006CB932103) and the Chinese Academy of Sciences.

Notes and references

1 J. E. Anthony, *Chem. Rev.*, 2006, **106**, 5028.
2 (*a*) K. Xiao, Y. Liu, T. Qi, W. Zhang, F. Wang, J. Gao, W. Qiu, Y. Ma, G. Cui, S. Chen, X. Zhan, G. Yu, J. Qin, W. Hu and D. Zhu, *J. Am. Chem. Soc.*, 2005, **127**, 13281; (*b*) J. G. Laquindanum, H. E. Katz and A. J. Lovinger, *J. Am. Chem. Soc.*, 1998, **120**, 664; (*c*) F. Valiyev, W. S. Hu, H. Y. Chen, M. Y. Kuo, I. Chao and Y. T. Tao, *Chem. Mater.*, 2007, **19**, 3018; (*d*) M. L. Tang, T. Okamoto and Z. N. Bao, *J. Am. Chem. Soc.*, 2006, **128**, 16002; (*e*) H. Ebata, E. Miyazaki, T. Yamamoto and K. Takimiya, *Org. Lett.*, 2007, **9**, 4499; (*f*) J. Gao, R. Li, L. Li, Q. Meng, H. Jiang, H. Li and W. Hu, *Adv. Mater.*, 2007, **19**, 3008; (*g*) B. Wex, B. R. Kaafarani, R. Schroeder, L. A. Majewski, P. Burckel, M. Grell and D. C. Neckers, *J. Mater. Chem.*, 2006, **16**, 1121.
3 (*a*) Y. Ma, Y. Sun, Y. Liu, J. Gao, S. Chen, X. Sun, W. Qiu, G. Yu, G. Cui, W. Hu and D. Zhu, *J. Mater. Chem.*, 2005, **15**, 4894; (*b*) Y. Wu, Y. Li, S. Gardner and B. S. Ong, *J. Am. Chem. Soc.*, 2005, **127**, 614; (*c*) S. Wakim, J. Bouchard, M. Simard, N. Drolet, Y. Tao and M. Leclerc, *Chem. Mater.*, 2004, **16**, 4386.
4 T. Qi, W. Qiu, Y. Liu, H. Zhang, X. Gao, Y. Liu, K. Lu, C. Du, G. Yu and D. Zhu, *J. Org. Chem.*, 2008, **73**, 4638.
5 H. Sirringhaus, R. H. Friend, C. Wang, J. Leuninger and K. Müllen, *J. Mater. Chem.*, 1999, **9**, 2095.
6 (*a*) H. E. Katz, Z. Bao and S. L. Gilat, *Acc. Chem. Res.*, 2001, **34**, 359; (*b*) A. Babel and S. A. Jenekhe, *Synth. Met.*, 2005, **148**, 169; (*c*) Y. Zhu, A. Babel and S. A. Jenekhe, *Macromolecules*, 2005, **38**, 7983.
7 A. W. Freeman, M. Urvoy and M. E. Criswell, *J. Org. Chem.*, 2005, **70**, 5014.
8 L. J. Pandya and B. D. Tilak, *J. Sci. Ind. Res.*, 1959, **18 B**, 516.
9 J. Samusakovics and E. Modest, *J. Am. Chem. Soc.*, 1950, **72**, 571.
10 T. Benincori, E. Brenna, F. Sannicolo, L. Trimarco, P. Antognazza, E. Cesarotti, F. Demartin and T. Pilati, *J. Org. Chem.*, 1996, **61**, 6244.
11 P. D. Clark, K. Clark, D. F. Ewing and R. M. Scrowston, *J. Chem. Soc., Perkin Trans. 1*, 1980, 677.
12 F. A. Carey, *Organic Chemistry*, McGraw-Hill Higher Education, Pergamon, 2000, 4th edn, p. 519, ch. 13.
13 R. Dabestani and I. N. Ivanov, *Photochem. Photobiol.*, 1999, **70**, 10.
14 M. He and F. Zhang, *J. Org. Chem.*, 2007, **72**, 442.
15 S. T. Bromley, M. Mas-Torrent, P. Hadley and C. Rovira, *J. Am. Chem. Soc.*, 2004, **126**, 6544.
16 (*a*) J.-L. Brédas, R. Silbey, D. S. Boudreaux and R. R. Chance, *J. Am. Chem. Soc.*, 1983, **105**, 6555; (*b*) J. Pommerehne, H. Vestweber, W. Guss, R. F. Mark, H. Bässler, M. Porsch and J. Daub, *Adv. Mater.*, 1995, **7**, 551; (*c*) M. Thelakkat and H.-W. Schmidt, *Adv. Mater.*, 1998, **10**, 219.